# Selective Loss of Smaller Spines in Schizophrenia

Matthew L. MacDonald, Ph.D., Jamil Alhassan, B.S., Jason T. Newman, Ph.D., Michelle Richard, B.S., Hong Gu, Ph.D., Ryan M. Kelly, B.S., Alan R. Sampson, Ph.D., Kenneth N. Fish, Ph.D., Peter Penzes, Ph.D., Zachary P. Wills, Ph.D., David A. Lewis, M.D., Robert A. Sweet, M.D.

**Objective:** Decreased density of dendritic spines in adult schizophrenia subjects has been hypothesized to result from increased pruning of excess synapses in adolescence. In vivo imaging studies have confirmed that synaptic pruning is largely driven by the loss of large or mature synapses. Thus, increased pruning throughout adolescence would likely result in a deficit of large spines in adulthood. Here, the authors examined the density and volume of dendritic spines in deep layer 3 of the auditory cortex of 20 schizophrenia and 20 matched comparison subjects as well as aberrant voltage-gated calcium channel subunit protein expression linked to spine loss.

**Method:** Primary auditory cortex deep layer 3 spine density and volume was assessed in 20 pairs of schizophrenia and matched comparison subjects in an initial and replication cohort (12 and eight pairs) by immunohistochemistry-confocal microscopy. Targeted mass spectrometry was used to quantify postsynaptic density and voltage-gated calcium channel protein expression. The effect of increased voltage-gated calcium channel subunit protein expression on spine density and volume was assessed in primary rat neuronal culture.

**Results:** Only the smallest spines are lost in deep layer 3 of the primary auditory cortex in subjects with schizophrenia, while larger spines are retained. Levels of the tryptic peptide ALFDFLK, found in the schizophrenia risk gene *CACNB4*, are inversely correlated with the density of smaller, but not larger, spines in schizophrenia subjects. Consistent with this observation, *CACNB4* overexpression resulted in a lower density of smaller spines in primary neuronal cultures.

**Conclusions:** These findings require a rethinking of the overpruning hypothesis, demonstrate a link between small spine loss and a schizophrenia risk gene, and should spur more in-depth investigations of the mechanisms that govern new or small spine generation and stabilization under normal conditions as well as how this process is impaired in schizophrenia.

*Am J Psychiatry 2017; 174:586–594; doi: 10.1176/appi.ajp.2017.16070814*

In 1982, Feinberg hypothesized that increased pruning of existing synapses during adolescence may contribute to the onset of schizophrenia (1), the incidence of which peaks toward the end of this developmental stage. Since then, increased synaptic pruning has become a major hypothesized pathogenic mechanism in schizophrenia, supported by the linking of two well-established observations. First, progressive gray matter loss has been observed in patients around the time of disease onset (2). Second, significant reductions in the density of dendritic spines on pyramidal neurons, the major postsynaptic sites of excitatory, glutamatergic synapses in the cerebral cortex, have consistently been observed in schizophrenia subjects in multiple brain regions within the frontal and temporal neocortex (3). As dendritic structural features are critical for signal processing (4–7), spine loss may then directly contribute to schizophrenia symptoms (3, 8).

Dendritic spines on cortical pyramidal neurons are highly plastic throughout all stages of development, with shifting rate constants of formation and loss governing the net spine population in each developmental epoch. Spine and synapse formation is most robust in the perinatal period, leading to a peak in synapse numbers at 2–4 years of age. These excess synapses are then "pruned," most intensely during adolescence, to adult levels. Throughout adulthood, large fractions of synapses are stably maintained, the physical incarnation of accumulated skills and memories (9–12). There is some turnover as skills and memories are lost, gained, or modified (13–15). In vivo imaging studies have confirmed the long-held view that adolescent pruning of dendritic spines is largely driven by elevated rates of elimination of mature or stable spines, while spine formation rates are similar to those seen in adulthood (14).

In vivo imaging studies have also found that mature or stable spines are larger, while new or transient spines are smaller (13, 15). Thus, the increase in synaptic pruning proposed to drive spine loss in schizophrenia should result in a deficit of larger spines in the adult cortex. Alternatively, recent genetic studies have implicated *N*-methyl-D-aspartate, brain-derived neurotrophic factor, calcium channel signaling,

*See related feature:* **Editorial** *by Dr. Coyle (p. 510)*

and mechanistic target of rapamycin signaling, which are pathways that are involved in spine formation and stabilization (16, 17). If spine loss in schizophrenia is driven by a decrease in the rate of new spine formation and stabilization, a decrease in the number of smaller spines would be expected. To test these alternate hypotheses, we used the colocalization of the postsynaptic density (PSD) protein spinophilin and the cytoskeleton protein filamentous-actin (F-actin) to assess, for the first time, both the density and volume of dendritic spines in schizophrenia.

**TABLE 1. Summary of Subject Characteristics in a Study of Selective Loss of Smaller Spines in Schizophrenia[a]**

| Characteristic | Comparison Group (N=20) | | Schizophrenia Group (N=20) | |
|---|---|---|---|---|
| | Mean | SD | Mean | SD |
| Age (years) | 45.8 | 11.3 | 46.9 | 13.7 |
| Postmortem interval (hours) | 16.4 | 16.7 | 17.0 | 7.9 |
| Storage time (months) | 131.8 | 38.2 | 124.4 | 35.9 |
| | N | % | N | % |
| Sex (female) | 7 | 35 | 7 | 35 |
| Right-handed[b] | 19 | 95 | 11 | 55 |
| Suicide | | | 4 | 20 |
| Schizoaffective disorder | | | 6 | 30 |
| Alcohol or substance abuse at time of death | | | 5 | 25 |
| Antipsychotic at time of death | | | 17 | 85 |

[a] There were no diagnostic group differences in age, sex, postmortem interval, storage time, or in the distribution of handedness between the diagnostic groups. The age ranges (in years) of the comparison and schizophrenia groups were 19–65 and 25–71, respectively. This cohort was previously reported in Shelton et al. (22).

[b] One subject in the comparison group was left-handed. In the schizophrenia group, five subjects were left-handed, one was ambidextrous, and handedness was unknown for three subjects.

## METHOD

### Human Subjects

We examined tissue from two cohorts (Table 1; see also Supplemental Table 1 in the data supplement that accompanies the online edition of this article), the first comprising 20 subjects diagnosed with schizophrenia or schizoaffective disorder (together referred to as schizophrenia), and the second comprising 20 comparison subjects matched on the basis of sex and as closely as possible for age, postmortem interval, and handedness (18–21). We have previously reported on spine density, but not spine density by spine volume, in these cohorts (22).

### Human Tissue Processing

At the University of Pittsburgh brain bank, the right and left hemispheres of postmortem brain are processed differently. Tissue blocks from the left hemisphere are fixed in paraformaldehyde, while blocks from the right hemisphere are fast-frozen in isopentane. Thus, tissue from the left hemisphere was used for immunohistochemistry, while tissue from the right hemisphere was used for targeted mass spectrometry.

### Immunohistochemistry

Tissue from the 20 pairs was divided into an initial cohort and a replication cohort: cohort 1 (N=12 pairs) and cohort 2 (N=8 pairs) (see Supplemental Table 2 in the online data supplement). These two cohorts were assayed independently. Tissue from each cohort was processed together across a series of immunohistochemical runs. To visualize dendritic spines, we used two markers in combination: a polyclonal antibody directed against spinophilin (Millipore AB5669, Billerica, Mass.), a protein that is highly enriched in spine heads, and the F-actin binding mushroom toxin phalloidin (Invitrogen A12380, Carlsbad, Calif.), which is also highly enriched in dendritic spines.

### Image Collection and Processing

Matched pairs from each cohort were imaged during the same session by an experimenter who was blind to diagnostic group. All images were taken using a confocal microscope equipped with a 60× oil supercorrected objective (equipment details are available in the online data supplement). Tissue thickness was measured at each sampling site and did not differ by diagnostic group ($F=0.05$, $df=1, 18.5$, $p=0.83$) or cohort ($F=2.35$, $df=1, 18.6$, $p=0.14$). Image stacks were taken beginning 12.5 μm below the tissue surface closest to the cover glass, stepping up 0.25 μm with each image until the tissue surface was reached. This procedure produced an image stack of 50 individual planes, each 512×512 pixels in size. Exposure times for 488-nm and 568-nm excitation wavelengths were set to optimize the spread of the intensity histogram for each cohort and then were kept consistent for all subjects within the cohorts.

Images were processed using SlideBook, version 5.027, with keystrokes automated by a software program (Automation Anywhere, San Jose, Calif.). Camera background was subtracted from channels 488 and 568 prior to processing. Underlying gray level values were extracted from the mask objects. See the data supplement for more detail on image processing.

### Calculation of Spine Density, Number, and Area

Although both spinophilin-immunoreactive and phalloidin binding are strongly localized to spines, each has some off-target label. Therefore, identification of putative dendritic spines required colocalization of spinophilin-immunoreactive and phalloidin label (Figure 1), operationalized as phalloidin mask objects that overlapped (≥1 voxel) with a spinophilin-immunoreactive mask object. Spine density

**FIGURE 1. Spine Attributes by Volume in a Study of Selective Loss of Smaller Spines in Schizophrenia**[a]

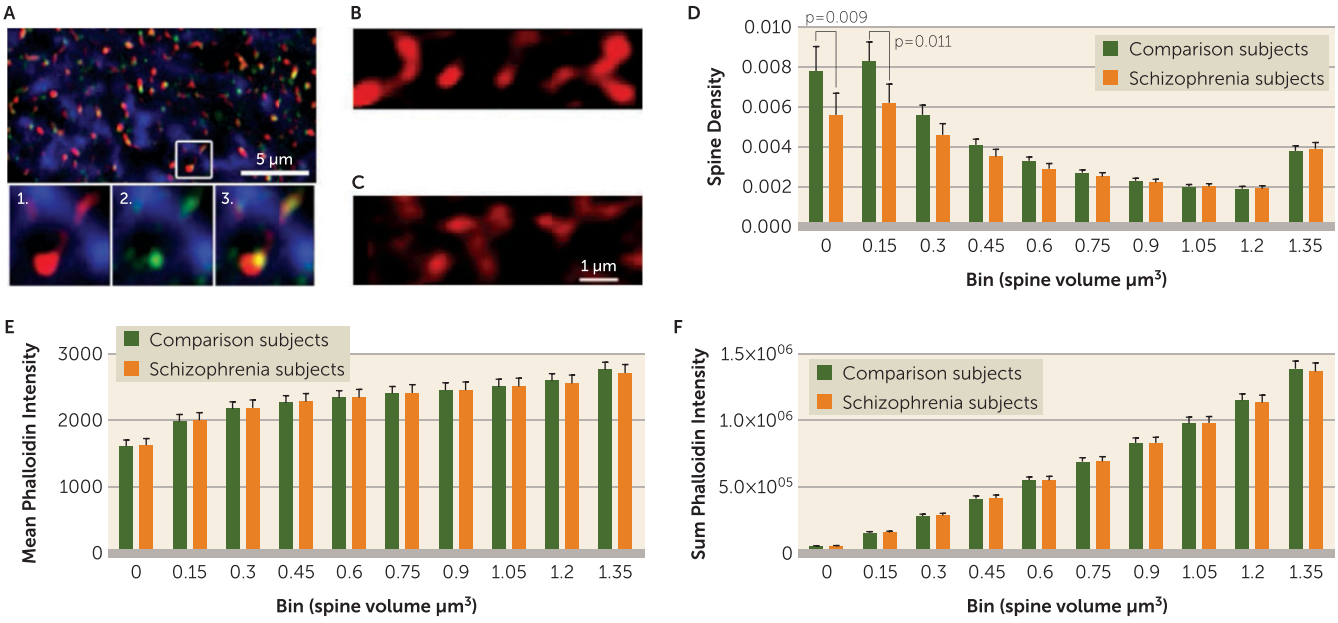


[a] Panel A displays phalloidin-labeled and spinophilin-immunoreactive puncta in deep layer 3 of the primary auditory cortex. In the top image, phalloidin-labeled puncta (red) and spinophilin-immunoreactive puncta (green) colocalize throughout deep layer 3 of Brodmann's area 41 and are found along microtubule-associated protein 2 immunoreactive processes (blue), suggesting spine structures along dendrites. The bottom images are a magnification of the inset in the top panel highlighting the relationship between phalloidin-labeled (1) and spinophilin-immunoreactive objects (2) and their colocalization in presumptive spine structures (3). The volume of phalloidin objects that colocalized with spinophilin was used to estimate spine volume. Panels B and C show representative phalloidin-labeled presumptive spines (60×) from a schizophrenia subject and a matched comparison subject, respectively. In Panel D, 20 pairs of subjects were assayed as an initial and as an independent replication cohort: cohort 1 (N=12 pairs) and cohort 2 (N=8 pairs) (see Supplemental Table 1 in the online data supplement). The results were equally significant in each cohort and are presented here as a single cohort for simplicity. The density of spines of different volumes (0.15 $\mu m^3$ increments, with the final bin including all objects with volume >1.35 $\mu m^3$) for comparison and schizophrenia subjects from both cohorts is shown. The density of spines in the bins of smaller volumes differed significantly between the comparison and schizophrenia groups (p values are Bonferroni corrected). Panel E displays the mean phalloidin intensity (calculated as the total phalloidin intensity of the spine object divided by spine object volume) of spines of different volumes from comparison and schizophrenia subjects. Panel F displays the sum phalloidin intensity of spines of different volumes from comparison and schizophrenia subjects. Mean and sum phalloidin intensity was consistent between the comparison and schizophrenia groups across all of the spine volume categories. Error bars indicate standard error of the mean.

($N_v$) in cohort 1 was calculated as previously described with minor modifications:

$$N_v := \frac{\bar{t}_{wQ^-}}{h} \cdot \frac{\sum\left(Q_i^- \cdot w_i\right)}{BA \cdot a \cdot \sum\left(P_i \cdot w_i\right)},$$

where $a$ is the area of the counting frames, $Q_i^-$ is the count of dendritic spines within the $i$th block, $P_i$ is the count of the associated points hitting the region of interest in the $i$th block, $h$ is the disector height (see the online data supplement for additional details), and $BA$ is the cryostat block advance (50 µm for cohort 1 and 60 µm for cohort 2). In addition, $\bar{t}_{wQ^-}$ is the block-and-number-weighted mean section thickness calculated using this formula:

$$\bar{t}_{wQ^-} := \frac{\sum\left(t_j \cdot q_j^- \cdot w_i\right)}{\sum\left(q_j^- \cdot w_i\right)},$$

where $t_j$ is the local section thickness measured centrally in the $j$th sampling frame and $q_j^-$ is the corresponding count of dendritic spines in the $j$th frame. In addition, $w_i$ is the block weight (i.e., either one or one-third). Because sections adjacent to the mapping sections were sampled for cohort 2, calculation of $N_v$ was made as described above but omitting the block weighting.

### Targeted Mass Spectrometry

Tissue homogenates were prepared from fresh frozen human A1 gray matter, described above and in the online data supplement. Total protein was extracted using SDS extraction buffer (0.125 M Tris–HCl [pH 7], 2% SDS and 10% glycerol) at 70°C. Protein concentration was measured using bicinchoninic acid assay (Micro BCA Protein Assay, Pierce). A pooled technical replicate sample composed of homogenate aliquots from all subjects was also prepared, and 20 µg of total protein from the gray matter homogenate or pooled sample was mixed with lysine $^{13}C_6$ stable isotope labeled neuronal proteome standard (23) ($^{13}C_6$ STD; 20 µg) for on-gel trypsin digestion. Samples were organized in a block distribution. Each block was run on a single 10-well 4%–12% BisTris gel with two SeeBlue Plus2 prestained protein standards (Invitrogen). On-gel trypsin digestion was performed as previously described (23), and samples were run 4 cm into the gel and divided into two fractions (above and below 65 $K_d$). Liquid chromatography–selected reaction monitoring mass

spectrometry assay development and implementation was performed as previously described (23, 24) (see the data supplement for details).

### Primary Neuronal Culture

Primary cortical neuronal cultures were prepared from embryonic day 17 Sprague-Dawley rats (Envigo and Charles River laboratories). Neurons were plated at 450,000 cells per well in 12-well plates. On day in vitro 12, the neurons were transfected with *CACNB4*/Myc (OriGene; catalog number RR204310) and green fluorescent protein (GFP) (gift of Ryan Logan, University of Pittsburgh). Thus, in the same plate some neurons were transfected with both constructs and some with only one. Neurons were fixed on day in vitro 15 for imaging with mouse anti-c-Myc antibody (1:1000, monoclonal 9E10; Santa Cruz Biotechnology) or with mouse anti-*CACNB4* (1:100, monoclonal S10–7; antibodies-online.com) and goat anti-c-Myc (1:100, polyclonal; Novus Biologicals). Image acquisition was performed on an Olympus (Center Valley, Pa.) BX51 WI upright microscope equipped with an Olympus spinning disk confocal (SDCM) using an Olympus PlanAPO N 10×0.40 NA air objective and a 1.42 numerical aperture 60× oil supercorrected objective.

Neurons were first categorized as either *CACNB4*-overexpressing or GFP-only controls based on c-Myc intensity. GFP-positive neurons on coverslips stained for both c-Myc and *CACNB4* were imaged at 10×. Exposure times for the 488 channel were optimized, whereas the 568 and 647 channels were shot at fixed exposures of 447 ms and 3,000 ms, respectively.

### Spine Counting and Masking

The TIFF files of all dendrites were imported into Stereo-Investigator (MicroBrightField) for counting. Protrusions from the dendritic shaft were manually assigned to one of the following categories, blind to experimental condition: short mushroom spine, long mushroom spine, short stubby spine, long stubby spine, or filopodia. Criteria for assignment have been previously described (25). Briefly, mushroom spines had distinct heads, while stubby spines did not. Long spines had a length greater than maximal width, and the rest were short. Filopodia were longer than 2 μm, thinner than 0.3 μm, and lacked a distinct head. For a given dendrite, the number of protrusions in each category was recorded, and the densities per μm of dendrite length for all spines, mushroom and stubby subtypes, and filopodia were calculated. A subset of the 60× dendritic images used for spine counting was randomly selected, blind to condition, for spine area analysis. In total, 35 GFP+ only dendrites and 38 Myc+/GFP+ dendrites were analyzed. Details on spine area calculation can be found in the data supplement.

### Statistical Analysis

*Human spine density by volume.* The data were analyzed through a linear mixed model with the pair effect taken into account. Spine density was assumed to be normally distributed. In the model, pair, cohort, diagnosis, and spine size category were the fixed effects. Subject was treated as a normal random effect to account for the repeated measures within each subject. Insignificant interaction terms were not included in the final model. The Kenward-Roger method was used to adjust for the denominator degrees of freedom. The analysis was implemented in SAS, version 9.4, with the PROC MIXED procedure. Categorical confounding effects were also assessed (see the data supplement).

*Human spine density continuous confounding effects.* For the analysis of continuous confounding effects, the percentage change of spine density within each pair was calculated as follows: $([C-S]/C) \times 100\%$. A simple linear regression analysis was done on each of the two confounding variables separately (age at onset and duration of disease). The slope of the percentage change of spine density on each confounding variable was estimated, and the p value to test whether the slope was significantly different from zero was provided in the table.

*Protein level correlations with spine density by size.* Pearson's correlation was used to determine the relationship between peptide expressions and spine density by volume.

## RESULTS

### Spine Density by Volume

As F-actin fills the spine (26), it can be used to estimate spine volume in immunohistochemical preparations of human postmortem brain tissue (Figure 1A through 1C). Thus, we estimated spine volumes in these subjects (Table 1; see also Supplemental Table 1 in the online data supplement) and calculated the density of spines by volume. The distribution of spine sizes we observed in the primary auditory cortex (A1) from comparison subjects (Figure 1D) was similar to previous reports from filled cells in the human cerebral cortex (27). Contrary to our hypothesis, we found that significant decreases in spine density were limited to the smallest spines (Figure 1D). Densities of medium and large spines were unaltered (Figure 1D). This effect was not associated with any potential confounding variables (see Supplemental Table 2 in the data supplement). Mean and total F-actin content per spine were unaffected in spines of all volumes (Figure 1E and 1F). The unchanged F-actin content per spine of small spines in schizophrenia indicates that the observed reduction in density was not due to decreased sensitivity of detection. This effect was not significantly associated with any confounding variables such as sex, medication history, or duration of disease (see Supplemental Table 2 in the data supplement).

### Voltage-Gated Calcium Channel Protein Expression

PSD and synaptic calcium signaling has been implicated in schizophrenia. Targeted mass spectrometry was used to quantify PSD and synaptic calcium signaling proteins in a subset of the subjects in which spine density was measured.

The expression of one tryptic peptide, ALFDFLK, was inversely correlated with the density of only smaller spines (Figure 2). It is important to note here that two subjects, one comparison subject and one subject with schizophrenia, had very high small spine densities (although the spine density for medium and large volume spines for these two individuals was similar to that of other subjects). Exclusion of these two outliers did not alter the association of reduced small spine density with schizophrenia. In addition, when these outliers were removed, we observed an even greater degree of correlation of ALFDFLK levels with small spine density (bin 1, $r=-0.55$, $p=0.0025$; bin 2, $r=-0.56$, $p=0.0021$; bin 3, $r=-0.51$, $p=0.0051$). ALFDFLK levels were not significantly increased in schizophrenia relative to comparison subjects. When subjects were separated by diagnosis, the correlation of ALFDFLK with small spine density was similar in comparison and schizophrenia subjects (Figure 2). In contrast, a module of PSD proteins we had previously identified as correlated with spine density in schizophrenia (24) did not demonstrate selectivity for small spines (data not shown).

### *CACNB4* Overexpression Alters Spine Density

To determine whether altered *CACNB4* expression could contribute to small spine loss, *CACNB4* was overexpressed in primary neuronal culture (Figure 3A and 3B). Total spine density was significantly decreased (Figure 3D). The density of filopodia, immature spine precursors, was unaltered (Figure 3E), suggesting that the reduced spine density observed was not the result of deficits in filopodia assembly. Further analysis of spine density by size (Figure 3C) revealed that loss was limited to smaller spines (Figure 3F).

## DISCUSSION

We observed that spine decreases in deep layer 3 of the primary auditory cortex in schizophrenia were limited to spines of smaller volumes. The decrease in small spines most likely reflects a reduction in the number of new or transient spines. The appearance of new or transient spines and their probability of stabilization are regulated by local calcium signaling generated by voltage-gated calcium channels (28, 29). Glutamate uncaging can also induce spinogenesis (12, 30), and the presence of a PSD is essential, but not sufficient, for new spine stabilization at a bouton (31). Genome-wide association (GWA) (17) and rare variant (16) analyses of schizophrenia have identified voltage-gated calcium channels and glutamate signaling from the PSD to the F-actin cytoskeleton in schizophrenia risk. It is important to note that the majority of small or new spines, even those that sample a bouton and acquire a PSD, are transient (31). Thus, even in healthy circuits, the early stages of spine stabilization are tentative, and the genetic factors that converge upon and destabilize PSD and voltage-gated calcium channel activity would likely have their greatest effect in these early, less robust stages of the spine life cycle.

An important consideration regards the potential effects of postmortem interval. We note that the cohorts in the spine density analysis were matched for postmortem interval as closely as possible. Furthermore, we did not observe any correlation between postmortem interval and small spine density (see Supplemental Table 2 in the online data supplement), strongly suggesting that postmortem interval does not affect our findings in schizophrenia relative to comparison subjects. Nevertheless, it is possible that postmortem interval could alter the relationship between spine size and spine class (i.e., stable or mature compared with new or transient), affecting our interpretation of the nature of the reduction in small spines in schizophrenia.

We sought to determine whether a link between PSD and/or voltage-gated calcium channel signaling proteins and small spine loss was present in these cohorts, finding that the expression of one tryptic peptide, ALFDFLK, was inversely correlated with the density of only smaller spines (Figure 2). The amino acid sequence ALFDFLK is unique to the four calcium channel beta subunits (*CACNB1* through *CACNB4*). Of these subunits, *CACNB2* and *CACNB4* have been implicated in schizophrenia pathogenesis by GWA (17) and rare variant (16) analyses. Of these two, *CACNB4* is the predominant isoform expressed in the adult temporal lobe (32, 33). In line with this observation in human tissue, we found that the overexpression of *CACNB4* decreased the density of smaller spines in primary neuronal culture. However, as ALFDFLK is present in other *CACNB* variants, it will be important to trace this effect to specific proteins.

*CACNB4*, like all voltage-gated calcium channel beta subunits, modulates the trafficking and biophysical properties of the alpha pore forming subunits (34). While the association of common and rare alleles of several voltage-gated calcium channel subunits with schizophrenia risk is well established (17, 35), a consensus on whether they result in a loss or gain of function, and on how they may exert an effect on synapses, is lacking (35). Our findings suggest that *CACNB4* overexpression depresses the calcium currents that drive spine formation and/or stabilization. Previous studies provide some potential mechanisms and precedent for this observed effect. *CACNB* proteins are required for voltage-dependent inactivation of calcium channels by a number of second messengers (36). Moreover, *CACNB4* knockout mice display evidence of increased calcium currents and increased excitability, manifest as epilepsy, suggesting that the dominant effect of *CACNB4* expression may be to reduce calcium currents (36). *CACNB4* is also noteworthy among the beta subunits in that it traffics from the synapse to the nucleus, affecting gene expression (37) and providing a second mechanism by which voltage-gated calcium channel activity could affect spine plasticity in addition to the regulation of local calcium signaling.

Despite identifying a significant correlation between ALFDFLK and small spine density, ALFDFLK levels were not significantly increased in our schizophrenia subjects. However, our in vitro data firmly demonstrate that increased

**FIGURE 2. Correlation of ALFDFLK With Spine Density by Bin in a Study of Selective Loss of Smaller Spines in Schizophrenia[a]**

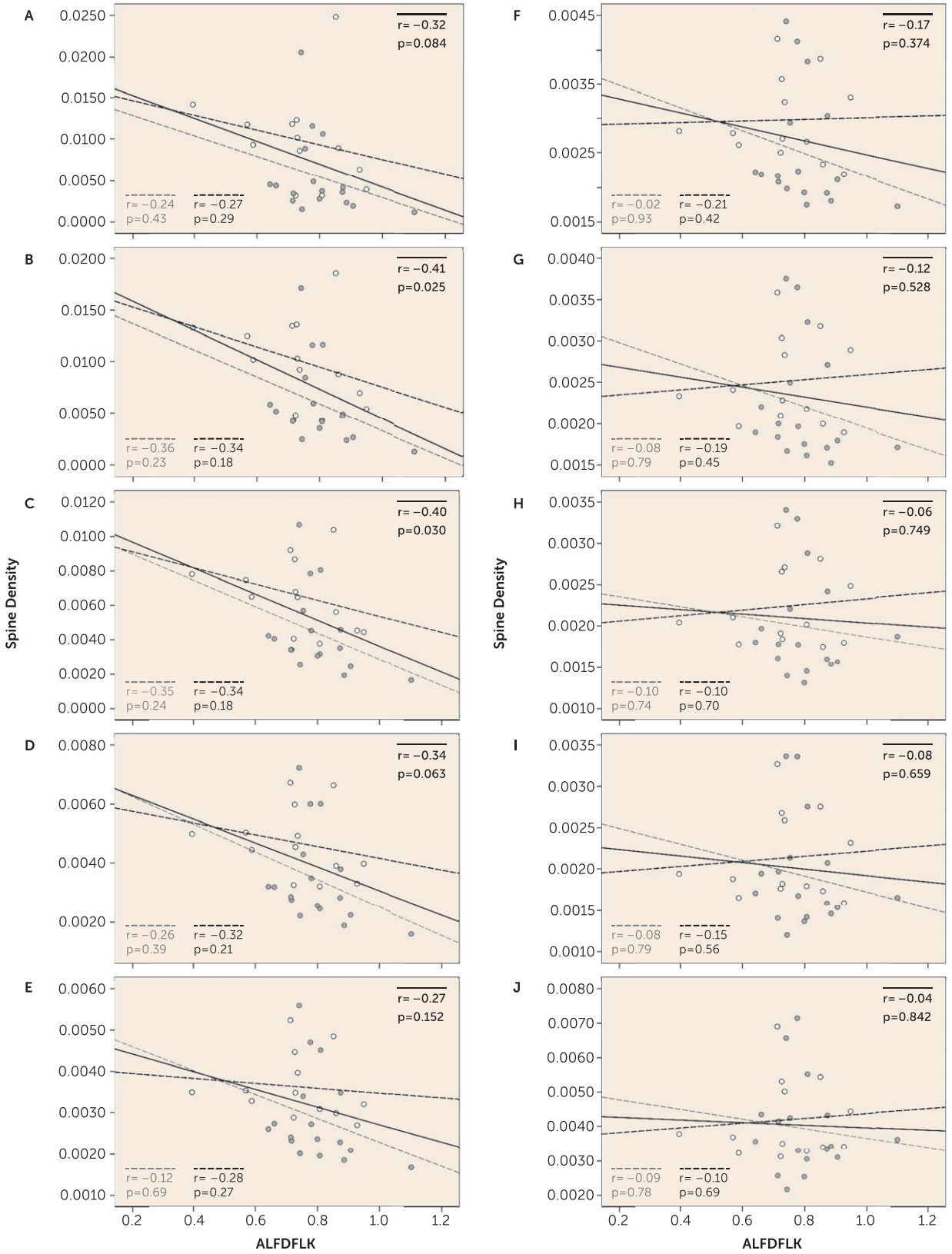


[a] The *CACNB* peptide ALFDFLK was quantified by liquid chromatography–selected reaction monitoring mass spectrometry. Expression of this peptide was plotted against the density of spine objects from each size bin. For example, panel A (0–0.15 $\mu m^3$) displays the correlation of ALFDFLK with the density of spine objects 0–0.15 $\mu m^3$ in both comparison (open black circle) and schizophrenia (filled gray circle) subjects. ALFDFLK expression was significantly inversely correlated with the density of small, but not medium or large, spines across all subjects (solid black line). This effect was similar for the comparison (black dashed line) and schizophrenia (gray dashed line) cohorts when separated.

**FIGURE 3. *CACNB4* Overexpression Decreases Small Spine Density in Primary Neuronal Culture**[a]

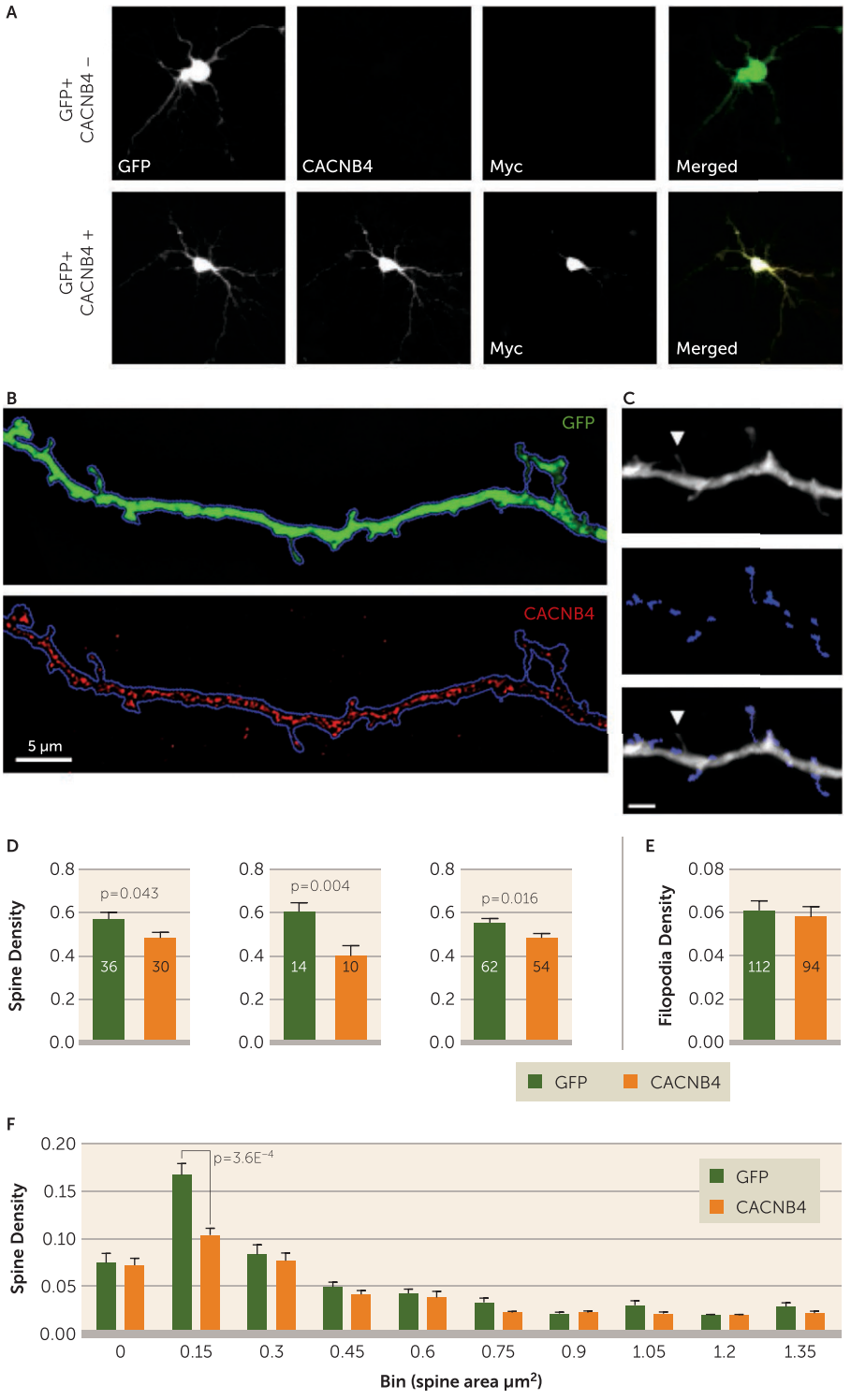


[a] Embryonic day 17 rat cortex primary neuronal cultures were transfected on day 12 with either green fluorescent protein (GFP) or GFP/*CACNB4*-Myc. Panel A displays representative 10× confocal images of transfected neurons. Endogenous *CACNB4* expression was not observed in these cultures, in line with previous reports that *CACNB4* is not expressed at this stage of development in the cortical cultures. *CACNB4* transfection induced robust somatodendritic expression (panel A) as well as expression in spines (panel B). Panel C displays processing for determination of dendritic spine volumes in another representative dendritic segment. Note that the filopodia is not masked. Spine and filopodia density was evaluated in three independent experiments. In each experiment, spine density was significantly decreased in *CACNB4*-expressing neurons (panel D). The number of dendrites assayed in each experiment is reported in each bar. In addition to reaching significance in each independent experiment, spine density was also significantly decreased across all three experiments ($p=6.5E^{-5}$). Panel E compares filopodia densities between GFP+ and GFP+/*CACNB4*-Myc+ neurons from all experiments, which were equivalent. Spine density was then assessed for spines of different sizes (panel F). A significant reduction in density selective for small spines was observed by two-way analysis of variance. The reported p value is Bonferroni corrected. Error bars indicate standard error of the mean.

*CACNB4* expression alone can drive small spine loss. This combination of findings is consistent with the current model for schizophrenia risk in which multiple genetic variants and epigenetic and environmental influences are believed to act in concert. No single gene or protein is believed to account for more than a small share of the population risk. As *CACNB4* interacts with and regulates multiple voltage-gated calcium channel subunits, many of which are also implicated in schizophrenia (17), it likely acts in concert with, or parallel to, other voltage-gated calcium channel genetic risk factors.

In the adult cortex, current evidence indicates that new or transient spines act as the substrate for reorganization of cortical networks in response to experience (38). These spines accomplish this rewiring both by providing for the formation of new persistent synapses (13, 15, 39) and by contributing to the destabilization of persistent synaptic spines through bouton competition (31, 40). Thus, a decrease in the rate of spine formation and/or their subsequent stabilization would result not only in their depletion but also in a decreased turnover rate of large spines by decreasing competitive loss, potentially explaining the observed conservation of large spines in schizophrenia despite a decrease in the small spines from which they are formed. The predicted cognitive consequences of new or transient spine reductions, in a general sense, would be impairments known to affect individuals with schizophrenia: deficits in new learning (41). Recently, auditory training exercises have shown promise for remediating auditory processing deficits in schizophrenia patients (42). Impairments in the generation or stabilization of new or transient spines in some subjects with schizophrenia may limit the available gains through such an approach. Thus, identification of therapeutics promoting small spine generation and stabilization might enhance the benefits of such training, providing a measurable outcome of drug efficacy.

In summary, our finding that A1 layer 3 spine loss in schizophrenia is limited to smaller spines strongly suggests that adult spine deficits result from a failure to generate and/or stabilize new or transient spines. This finding requires a rethinking of the overpruning hypothesis and should spur a more in-depth investigation of the mechanisms that govern spinogenesis, spine stabilization, and their role in schizophrenia. As a first step, we have identified one such mechanism, *CACNB4* expression levels, which could contribute in part to the loss of small spines in schizophrenia. Future studies to confirm the effect of *CACNB4* and other *CACNB* subunits in vivo are warranted and might include direct observation of spine dynamics. In addition, the pleiotropic genetic associations of calcium channel subunits with schizophrenia risk highlight the continued need to expand investigations beyond single proteins to the larger signaling network to enhance understanding of how genetic risk is translated into synaptic pathology.

## AUTHOR AND ARTICLE INFORMATION

From the Departments of Psychiatry, Neurology, Statistics, and Neurobiology, Translational Neuroscience Program, University of Pittsburgh School of Medicine, Pittsburgh; the Mental Illness Research, Education, and Clinical Center, VA Pittsburgh Healthcare System, Pittsburgh; and the Departments of Physiology and of Psychiatry and Behavioral Sciences, Northwestern University Feinberg School of Medicine, Chicago.

Address correspondence to Dr. Sweet (sweetra@upmc.edu).

Presented at the annual meeting of the American College of Neuropsychopharmacology, Hollywood, Fla., Dec. 7, 2015; at the fourth annual meeting of the Molecular Psychiatry Association, Maui, Hawaii, Oct. 9, 2016; at the annual meeting of the American College of Neuropsychopharmacology, Hollywood, Fla., Dec. 7, 2016; and at the 50th Winter Conference on Brain Research, Big Sky, Mont., Jan. 31, 2017.

Supported by NIMH grants MH-107756 to Dr. MacDonald, MH-096985 to Dr. Fish, MH-071316 and MH-097216 to Dr. Penzes, and MH-071533 to Dr. Sweet. Dr. MacDonald is also supported by a NARSAD Young Investigator Award from the Brain and Behavior Research Foundation.

The authors thank Dr. C. Sue Johnston for assistance with the clinical data, Mary Brady for design assistance, and the research staff of the Translational Neuroscience Program for technical assistance.

The content of this article is solely the responsibility of the authors and does not represent the official views of NIMH, NIH, the VA, or the U.S. government.

Dr. Lewis currently receives investigator-initiated research support from Pfizer. In 2013–2015, he served as a consultant in the areas of target identification and validation and new compound development to Autifony, Bristol-Myers Squibb, Concert Pharmaceuticals, and Sunovion. The other authors report no financial relationships with commercial interests.

Received July 20, 2016; revision received Dec. 19, 2016; accepted Jan. 9, 2017; published online March 31, 2017.

## REFERENCES

1. Feinberg I: Schizophrenia: caused by a fault in programmed synaptic elimination during adolescence? J Psychiatr Res 1982–1983; 17:319–334
2. Vita A, De Peri L, Deste G, et al: Progressive loss of cortical gray matter in schizophrenia: a meta-analysis and meta-regression of longitudinal MRI studies. Transl Psychiatry 2012; 2:e190
3. Moyer CE, Shelton MA, Sweet RA: Dendritic spine alterations in schizophrenia. Neurosci Lett 2015; 601:46–53
4. Chen X, Leischner U, Rochefort NL, et al: Functional mapping of single spines in cortical neurons in vivo. Nature 2011; 475:501–505
5. Midtgaard J: The integrative properties of spiny distal dendrites. Neuroscience 1992; 50:501–502
6. Shepherd GM, Woolf TB, Carnevale NT: Comparisons between active properties of distal dendritic branches and spines: implications for neuronal computations. J Cogn Neurosci 1989; 1:273–286
7. Tsay D, Yuste R: On the electrical function of dendritic spines. Trends Neurosci 2004; 27:77–83
8. Penzes P, Cahill ME, Jones KA, et al: Dendritic spine pathology in neuropsychiatric disorders. Nat Neurosci 2011; 14:285–293
9. Attardo A, Fitzgerald JE, Schnitzer MJ: Impermanence of dendritic spines in live adult CA1 hippocampus. Nature 2015; 523:592–596
10. Yang G, Pan F, Gan WB: Stably maintained dendritic spines are associated with lifelong memories. Nature 2009; 462:920–924
11. Chen CC, Lu J, Zuo Y: Spatiotemporal dynamics of dendritic spines in the living brain. Front Neuroanat 2014; 8:28
12. Hayashi-Takagi A, Yagishita S, Nakamura M, et al: Labelling and optical erasure of synaptic memory traces in the motor cortex. Nature 2015; 525:333–338
13. Knott G, Holtmaat A: Dendritic spine plasticity: current understanding from in vivo studies. Brain Res Rev 2008; 58:282–289
14. Zuo Y, Lin A, Chang P, et al: Development of long-term dendritic spine stability in diverse regions of cerebral cortex. Neuron 2005; 46: 181–189
15. Holtmaat AJ, Trachtenberg JT, Wilbrecht L, et al: Transient and persistent dendritic spines in the neocortex in vivo. Neuron 2005; 45: 279–291

16. Purcell SM, Moran JL, Fromer M, et al: A polygenic burden of rare disruptive mutations in schizophrenia. Nature 2014; 506:185–190
17. Schizophrenia Working Group of the Psychiatric Genomics Consortium: Biological insights from 108 schizophrenia-associated genetic loci. Nature 2014; 511:421–427
18. Akil M, Pierri JN, Whitehead RE, et al: Lamina-specific alterations in the dopamine innervation of the prefrontal cortex in schizophrenic subjects. Am J Psychiatry 1999; 156:1580–1589
19. Moyer CE, Delevich KM, Fish KN, et al: Reduced glutamate decarboxylase 65 protein within primary auditory cortex inhibitory boutons in schizophrenia. Biol Psychiatry 2012; 72:734–743
20. Moyer CE, Delevich KM, Fish KN, et al: Intracortical excitatory and thalamocortical boutons are intact in primary auditory cortex in schizophrenia. Schizophr Res 2013; 149:127–134
21. Sweet RA, Henteleff RA, Zhang W, et al: Reduced dendritic spine density in auditory cortex of subjects with schizophrenia. Neuropsychopharmacology 2009; 34:374–389
22. Shelton MA, Newman JT, Gu H, et al: Loss of microtubule-associated protein 2 immunoreactivity linked to dendritic spine loss in schizophrenia. Biol Psychiatry 2015; 78:374–385
23. MacDonald ML, Ciccimaro E, Prakash A, et al: Biochemical fractionation and stable isotope dilution liquid chromatography-mass spectrometry for targeted and microdomain-specific protein quantification in human postmortem brain tissue. Mol Cell Proteomics 2012; 11:1670–1681
24. MacDonald ML, Ding Y, Newman J, et al: Altered glutamate protein co-expression network topology linked to spine loss in the auditory cortex of schizophrenia. Biol Psychiatry 2015; 77:959–968
25. Richardson RJ, Blundon JA, Bayazitov IT, et al: Connectivity patterns revealed by mapping of active inputs on dendrites of thalamorecipient neurons in the auditory cortex. J Neurosci 2009; 29:6406–6417
26. Hotulainen P, Hoogenraad CC: Actin in dendritic spines: connecting dynamics to function. J Cell Biol 2010; 189:619–629
27. Benavides-Piccione R, Fernaud-Espinosa I, Robles V, et al: Age-based comparison of human dendritic spine structure using complete three-dimensional reconstructions. Cereb Cortex 2013; 23:1798–1810
28. Sheng L, Leshchyns'ka I, Sytnyk V: Neural cell adhesion molecule 2 promotes the formation of filopodia and neurite branching by inducing submembrane increases in $Ca^{2+}$ levels. J Neurosci 2015; 35: 1739–1752
29. Lohmann C, Bonhoeffer T: A role for local calcium signaling in rapid synaptic partner selection by dendritic filopodia. Neuron 2008; 59: 253–260
30. Kwon HB, Sabatini BL: Glutamate induces de novo growth of functional spines in developing cortex. Nature 2011; 474:100–104
31. Cane M, Maco B, Knott G, et al: The relationship between PSD-95 clustering and spine stability in vivo. J Neurosci 2014; 34:2075–2086
32. Wu C, Orozco C, Boyer J, et al: BioGPS: an extensible and customizable portal for querying and organizing gene annotation resources. Genome Biol 2009; 10:R130
33. http://biogps.org/
34. Dolphin AC: Calcium channel auxiliary α2δ and β subunits: trafficking and one step beyond. Nat Rev Neurosci 2012; 13:542–555
35. Heyes S, Pratt WS, Rees E, et al: Genetic disruption of voltage-gated calcium channels in psychiatric and neurological disorders. Prog Neurobiol 2015; 134:36–54
36. Buraei Z, Yang J: Structure and function of the β subunit of voltage-gated $Ca^{2+}$ channels. Biochim Biophys Acta 2013; 1828:1530–1540
37. Etemad S, Obermair GJ, Bindreither D, et al: Differential neuronal targeting of a new and two known calcium channel β4 subunit splice variants correlates with their regulation of gene expression. J Neurosci 2014; 34:1446–1461
38. Fu M, Yu X, Lu J, et al: Repetitive motor learning induces coordinated formation of clustered dendritic spines in vivo. Nature 2012; 483:92–95
39. Knott GW, Holtmaat A, Wilbrecht L, et al: Spine growth precedes synapse formation in the adult neocortex in vivo. Nat Neurosci 2006; 9:1117–1124
40. Barnes SJ, Cheetham CE: A role for short-lived synapses in adult cortex? J Neurosci 2014; 34:7044–7046
41. Saykin AJ, Shtasel DL, Gur RE, et al: Neuropsychological deficits in neuroleptic naive patients with first-episode schizophrenia. Arch Gen Psychiatry 1994; 51:124–131
42. Fisher M, Herman A, Stephens DB, et al: Neuroscience-informed computer-assisted cognitive training in schizophrenia. Ann N Y Acad Sci 2016; 1366:90–114